Hindawi Publishing Corporation
Physics Research International
Volume 2010, Article ID 164249, 14 pages
doi:10.1155/2010/164249

Review Article

Inductively Coupled Plasma Sources and Applications

Tomohiro Okumura

Production Engineering Laboratory, Panasonic Corporation, 2-7, Matsuba-Cho, Kadoma, Osaka 571-8502, Japan

Correspondence should be addressed to Tomohiro Okumura, okumura.tomohiro@jp.panasonic.com

Received 22 October 2010; Accepted 30 December 2010

Academic Editor: Lorenzo Pavesi

Copyright © 2010 Tomohiro Okumura. This is an open access article distributed under the Creative Commons Attribution License, which permits unrestricted use, distribution, and reproduction in any medium, provided the original work is properly cited.

The principle of inductively coupled plasma (ICP) and perspective of ICP development are reviewed. Multispiral coil ICP (MSC-ICP), which has the advantages of low inductance, high efficiency, and excellent uniformity, is discussed in detail. Applications to thin film processing technologies and the future prospects of ICP are also described.

1. Introduction

In the 1990s, thin-film processing technologies using low-pressure high-density plasma (HDP) sources rapidly improved as manufacturing techniques for electronic devices such as semiconductors and liquid crystal displays (LCDs). Progress in these areas continues today.

Plasma generation in a low-pressure etching chamber decreases the probability that ions will collide with one another or with neutral gas particles in an ion sheath, which is formed near the substrate surface, with the result that ions are uniformly directed toward the substrate. The use of highly ionized HDP increases the ratio of ions to neutral radicals reaching the substrate, enhancing etching anisotropy. Microprocessing with a high aspect ratio is therefore possible. In plasma chemical vapor deposition (CVD), a fine pattern is filled flat, owing to the sputtering effect of ions, thus achieving deposition with a high aspect ratio.

Moreover, there is an advantage of independent controllability of plasma density and bias energy in the HDP process, in which it is possible to control the plasma density by adjusting the source power, and the self bias voltage by the bias power. Self bias voltage is a key parameter related to ion energy radiated on the substrate.

These features of HDP are well known from the past. Electron cyclotron resonance plasma (ECRP), invented in 1970s, had been only one practical HDP and occupied an important position for a long time. However, the strong magnetic field needed by ECRP and the resulting separation of charged particles can cause electrostatic damage to devices. ECRP has the disadvantage of a complex chamber configuration. It was clear that a simply configured HDP without a static magnetic field was strongly needed.

Inductively coupled plasma (ICP) sources meeting these demands started to be investigated in the 1990s, eventually becoming widely used in semiconductor manufacturing. In this paper, the principle of ICP and perspective of ICP development are reviewed by presenting various ICPs. Also discussed in detail is multispiral coil ICP (MSC-ICP), invented by the authors. Lastly, applications to thin-film processing technologies and finally the future prospects of ICP are examined.

2. Principle of Inductively Coupled Plasma

An electromagnetic field created by radio frequency (RF) current flowing in a coil plays an important role in ICP. Figure 1 shows the RF magnetic field (B-field) and RF electric field (E-field) created inside the plasma chamber by applying RF power to the planar coil through the dielectric window [1]. The main energy absorption mechanism in ICP is Joule heating, in which electrons accelerated by the E-field collide numerous times with other particles. The voltage drop per unit length equals the electric field E, and the electron drift velocity equals $\mu_e E$ (μ_e is electron mobility), so the Joule heating power P_j is expressed as

$$P_j = e n_e \mu_e E^2, \tag{1}$$

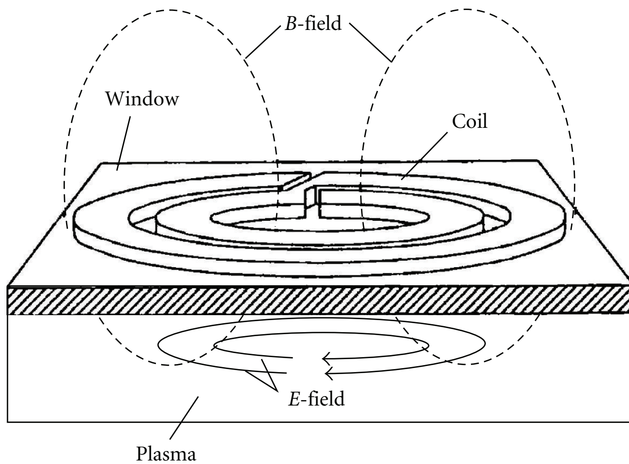

Figure 1: RF magnetic field (B-field) and RF electric field (E-field) created inside the plasma chamber by applying RF power to the planar coil through the dielectric window [1].

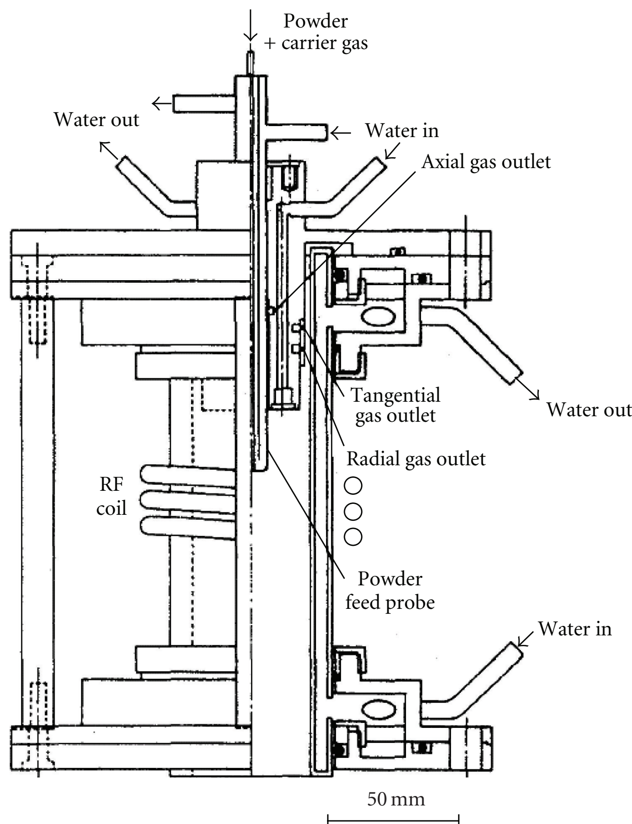

Figure 2: Cross-sectional view of ICP spray coating equipment [2].

where e is the electron charge and n_e is the electron density.

Stochastic heating by anomalous skin effects is also important as another energy absorption mechanism in ICP because HDP can be maintained at very low, collisionless pressure [3]. Anomalous skin effect means heating without collision. If the mean free path of an electron is sufficiently larger than the skin depth of the electromagnetic field, then electrons penetrating into the skin region δ depth under the dielectric window can receive energy from the electromagnetic field. When the excitation angular frequency ω is sufficiently larger than the elastic collision frequency ν, skin depth δ is written as

$$\delta = \frac{c}{\omega_{pe}}, \tag{2}$$

where c is the speed of light, and ω_{pe} is the electron plasma angular frequency. In processing, plasma δ can be roughly estimated on the order of mm to cm. Equation (2) is based on the hypothesis that electrons have very small energy and create no thermal motion. If the collision frequency ν becomes so small at low pressure that ω and ν are much smaller than $\nu/2\delta$, then the time scale of interaction between electrons and the electric field, while electrons are in the skin region becomes shorter than that of electromagnetic field fluctuation and collisions. As a result, electrons accelerating inside the skin region can return to bulk plasma without losing their kinetic energy and thus contribute to ionization.

3. Perspective of Inductively Coupled Plasma Development

ICP was first used as a thermal plasma in the coating field in the 1960s, long before ICP began being used in semiconductor processing. Figure 2 is a cross-sectional view of ICP spray coating equipment [2]. Thermal plasma (more than 10,000 K) can be generated inside the water-cooled quartz tube by supplying RF power to the coil arranged around the tube. When the powders are injected into the plasma with carrier gas, melting powders are project into the work, creating a film of functional material on it. An ICP torch has been also used in the field of optical emission spectroscopy. Operating at pressures of 10,000 Pa or more and with a typical diameter of several mm to cm, these thermal ICP torches had little to do with thin film processing dealing with large semiconductor wafers, with diameters of more than 100 mm requiring a vacuum of 0.1 to 100 Pa.

In the early 1990s, IBM and Lam Research released planar ICP, which attracted attention as a newly developed low-pressure HDP for semiconductor manufacturing. Figure 3 shows the ICP developed by IBM [4], and Figure 4, by Lam [5]. In both cases, a planar coil is arranged on top of the dielectric window. In Figure 3, permanent magnets are arranged inside the plasma chamber in order to confine the plasma for improved uniformity in plasma density distribution. However, it is well known that uniform plasma can be easily achieved without a magnetic field by optimizing the coil shape, so ICPs for semiconductor mass production generally have no magnetic field.

Power efficiency is very important in ICP. Reports have shown that a thick dielectric window decreases power efficiency [17] because mutual inductance between the coil and plasma decreases, resulting in increased current flowing through the coil and the increased copper loss.

Multi-spiral coil ICP with easy RF matching accomplished by decreasing the coil inductance consistent with

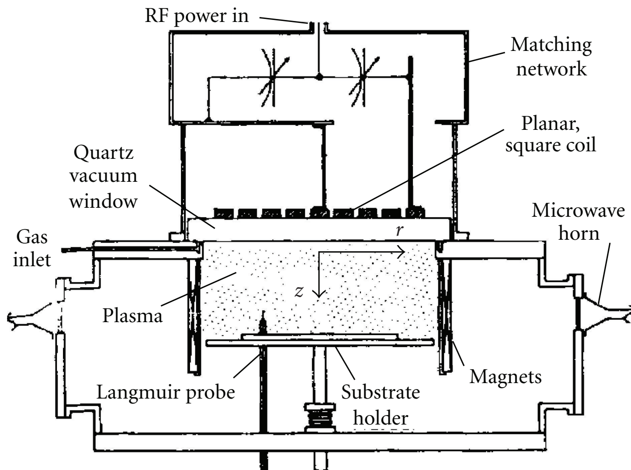

Figure 3: ICP developed by IBM [4].

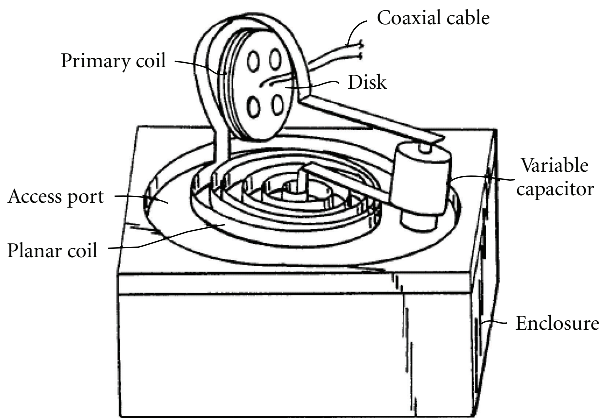

Figure 4: ICP developed by Lam [5].

excellent uniformity was put to practical use by the authors. This will be described later in detail.

An effective way of suppressing capacitive coupling between the coil and plasma is to insert a Faraday shield as shown in Figure 5 [6]. The Faraday shield helps prevent deterioration of the dielectric window by ion bombardment, which is caused by self bias charging in the dielectric window. Reports also indicate that favorable anisotropic etched profiles in the gate etching process can be achieved by suppressing oxygen derived from the dielectric window [18].

Conversely, etching of nonvolatile material is achieved by actively supplying RF power to the Faraday shield and etching the dielectric window at the same time, as illustrated in Figure 6 [7]. Figure 7 shows photos of quartz domes before and after etching 50 wafers with platinum film [7]. The reactivity of platinum is so poor that large amounts of conducting platinum film deposit on the inner surface of the quartz dome when the Faraday shield is grounded. Because this film shields the electromagnetic field created by the coil, the discharge cannot be maintained. However, in the case of Figures 6 and 7, preventing platinum film deposition on the quartz dome was successful. The PZT etching device shown in Figure 8 also utilizes the same function [8].

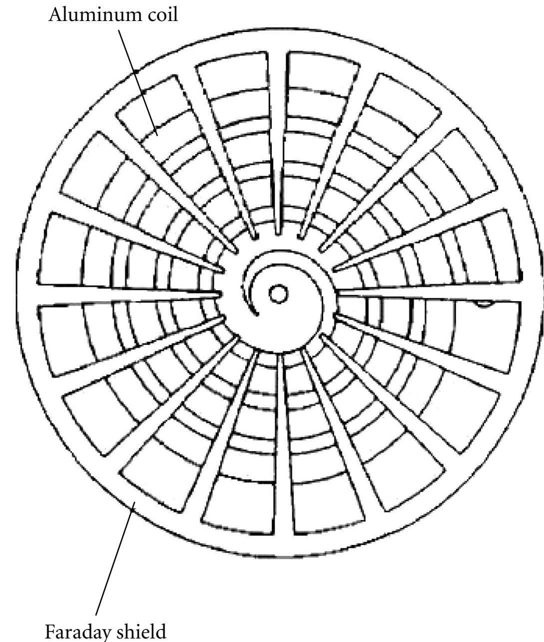

Figure 5: Faraday shield [6].

Thus, ICP continues evolved to meet various needs, and now is used overwhelmingly in gate-etch and metal-etch applications. However, ICP has not become widely used in the dielectric-etch process. This is due to the low etching selectivity to silicon under the dielectric. In ICP, the gap between the dielectric window and substrate must be wide (approx. 100 mm) in order to keep uniformity, but this results in larger chamber volume and longer residence time of gases in the chamber; thus reactive gas dissociation rapidly progresses. To resolve this issue, ICP has been developed with inner and outer coils that enable generation of a uniform plasma in a narrow gap configuration by independently applying RF power to each coil, as illustrated in Figure 9 [9].

Also developed, though for controlling the planned distribution of plasma density, not to create a narrower gap, is an ICP with an inner and outer coil that enables processing of large semiconductor wafers by independently applying RF power to each coil, as shown in Figure 10 [10].

Internal coil type ICP (IC-ICP), in which a coil is installed inside the plasma chamber without a dielectric window, has been investigated. IC-ICP requires a dielectric coating onto a coil to prevent the coil, a conductor, from directly contacting the plasma. The thickness of the coating can be so thin (<1 mm) that high power efficiency can be obtained. Figure 11 shows an example of IC-ICP, in which direct current (DC) introduced together with RF current to a coil creates a DC magnetic field around the coil. The DC magnetic field decreases charging on the coil's surface, protecting the dielectric coating from ion bombardment [11]. As shown in Figure 12, another IC-ICP has also been

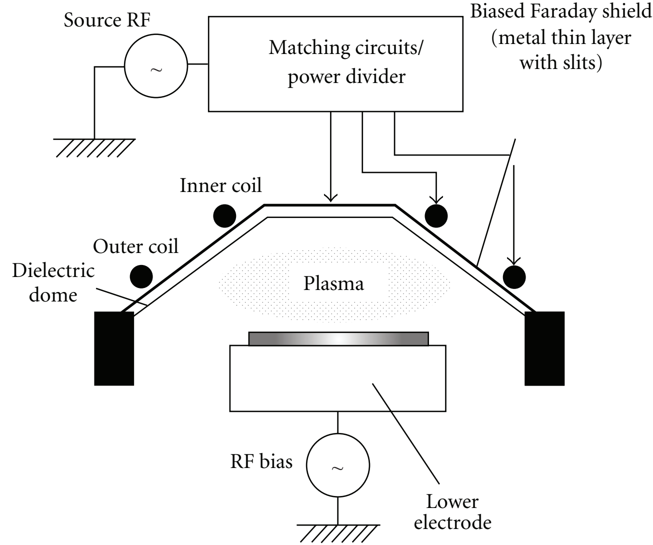

Figure 6: Etcher actively supplying RF power to the Faraday shield [7].

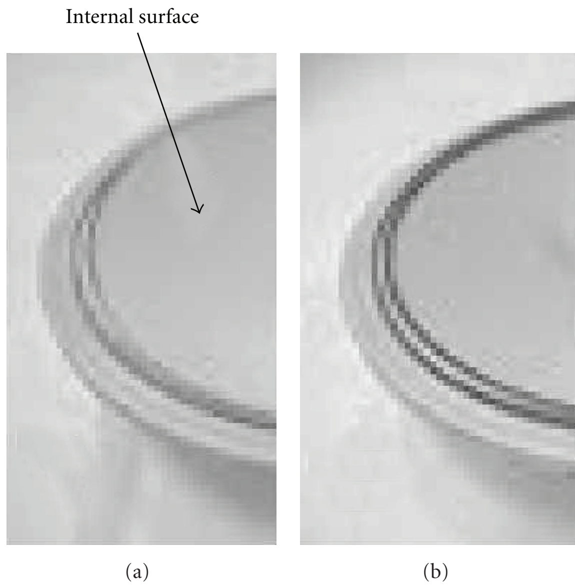

Figure 7: Photos of quartz domes: (a) before and (b) after etching 50 wafers with platinum film [7].

developed with several internal coils inside the chamber to realize large area ICP [12].

4. Multispiral Coil ICP

4.1. Concept. Considering the requirements for large area and uniform plasma generation, the coil shape was studied. Uniformly flowing linear current I on a small length l with angular frequency of ω is equivalent to an electric dipole of $Il/j\omega$ in moment. The θ component of the electric field radiated from dipole E_θ is expressed as

$$E_\theta = \frac{Ile^{-jkr}}{j4\pi\omega\varepsilon}\left(\frac{1}{r^3} + \frac{jk}{r^2} + \frac{k^2}{r}\right)\sin\theta, \quad (3)$$

where $k^2 = \omega^2\mu\varepsilon - j\omega\mu\sigma$ and μ, ε, and σ are magnetic permeability, permittivity and conductivity of the medium, respectively [27]. Variable r is the distance from the center of the linear current. In (3), the terms of r^{-3}, r^{-2}, and r^{-1} are known as the quasielectrostatic field, induction field, and radiation field, respectively. The induction field, important in ICP, is in inverse proportion to the square of the distance from the coil; thus the coil and plasma are coupled strongly through the dielectric window. This fact indicates that the coil shape greatly affects plasma distribution. In other words, to perform a uniform process, a large-diameter coil should be formed in multiple turns onto the dielectric window positioned on the opposite side of the wafer.

However, coil inductance can be increased not only by increasing the coil turns but also by increasing the coil diameter. Generally, in RF transmission network the characteristic impedance is adjusted at 50 Ω. Fine RF matching requires a coil of less than 250 Ω inductance.

The inductance of a single-spiral coil (SSC) is examined. The inductance L_A of an SSC of N number of turns is given as

$$L_A = \sum_{i=1}^{N} M_s\left(l_i, l_i - (w_c + t_c)e^{-1.5}\right) + 2\sum_{i=1}^{N-1}\sum_{j=i+1}^{N} M_s\left(l_i, l_j\right),$$

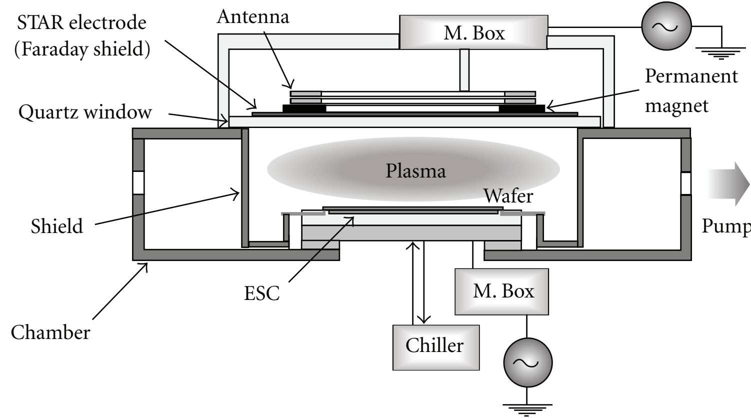

FIGURE 8: PZT etching device with a Faraday shield [8].

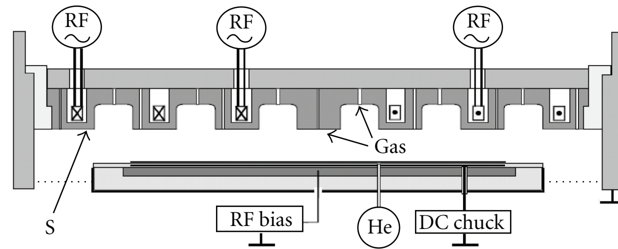

FIGURE 9: ICP with inner and outer coils that enable generation of uniform plasma by independently applying RF power to each coil [9].

$$
\begin{aligned}
M_s &= \frac{\mu_0\left(l_i + l_j\right)}{\pi} \\
&\quad \times \left[\ln \frac{\sqrt{k_{ij}^2 + 1} + 1}{k_{ij}} - k_{ij} \ln\left(\sqrt{k_{ij}^2 + 1} + k_{ij}\right) \right. \\
&\quad \left. + \left(k_{ij} + 1\right) \left\{ \sqrt{2} - \ln\left(\sqrt{2} + 1\right) \right\} - 2\sqrt{k_{ij}^2 + 1} \right], \\
k_{ij} &= \frac{l_i - l_j}{l_i + l_j}, \\
l_i &= l_c - w_c - 2(i - 1)(w_c + d_c),
\end{aligned} \tag{4}
$$

where w_c is the width of the coil, d_c is the width of the intervals of the coil, t_c is the thickness of the coil, l_c is the side length of the outermost conductor (see Figure 13), l_i is the length of conductor i, and $M_s(l_i, l_j)$ is the self inductance of each conductor if $i = j$ and the mutual inductance between conductors i and j if $i \neq j$ [13].

Figure 14 shows that the relationship between the calculated inductance and the outer length of a rectangular SSC, where N, w_c, d_c, and t_c are 4, 5 mm, 20 mm, and 10 mm, respectively. If the wafer diameter is 200 mm, the outer length of a coil diameter should be larger than 300 mm, with the coil inductance of the SSC reaching almost 4 μH (= 340 Ω). A larger coil enlarges its own inductance; thus, fine RF matching and uniform plasma generation would be incompatible.

The authors first tested plural coils arranged on a dielectric window to form a parallel circuit as illustrated in Figure 15. It was intended that all the coils contribute to plasma generation. Figure 16 shows the measured inductance, and plasma density as a function of the number of coils. This graph indicates that increasing the number of coils leads to decreased inductance, and that plasma density drops at the same time. This is probably due to cancellation of the electromagnetic field radiated from the neighboring coil.

To solve this problem, MSC-ICP was proposed as shown in Figure 17, in which multiple spiral coils are connected in parallel without each coil cancelling the electromagnetic field radiated from another [14]. In the chamber, each coil generates an overlapping RF electromagnetic field. Even with 1 to 2 turns of each coil, if the multiplicity is 4, for example, the MSC produces an effect for the in-plane uniformity of plasma equivalent to that of an SSC with 4 to 8 turns. That is, using an MSC makes it possible to create an ICP coil with remarkably smaller inductance than that of conventional SSC systems.

4.2. Basic Characteristics of MSC-ICP. Figure 18 shows the configuration of the experimental apparatus [14]. A quartz plate as a dielectric window with an MSC was set atop a vacuum chamber facing a single-crystal silicon wafer of 200 mm diameter. Ion-saturated current density was measured at a point 5 mm above the wafer, using a Langmuir probe.

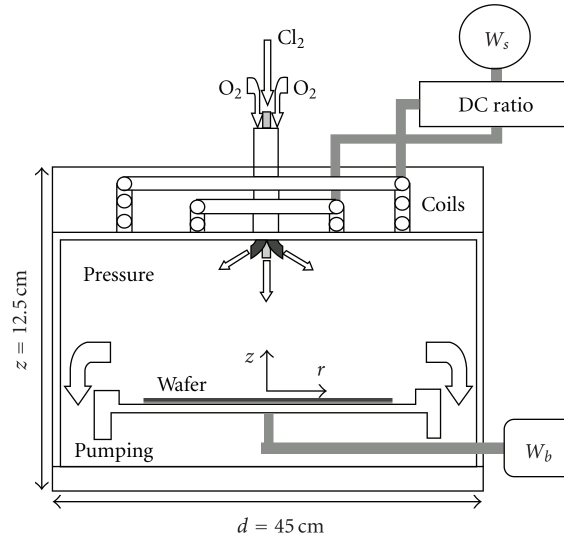

Figure 10: ICP with inner and outer coils that enable generation of uniform plasma by independently applying RF power to each coil [10].

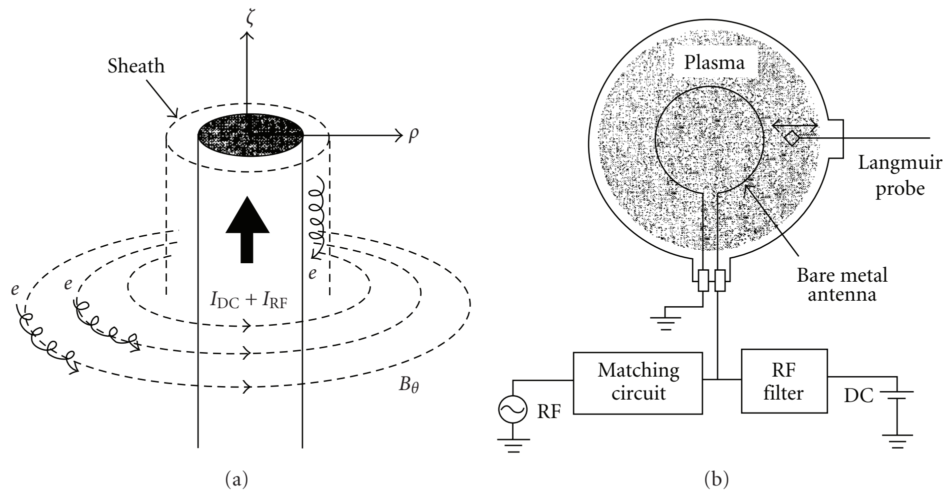

Figure 11: Example of IC-ICP, in which direct current introduced with RF current to a coil creates a direct-current magnetic field around the coil [11].

Figure 19 shows the relation between inductance and the number of multiple spiral coils [14]. As Figure 19 shows, inductance can be decreased by increasing the number of spirals. The inductance of a four-spiral coil is about 57% that of a coil with one spiral.

Figures 20 and 21 show ion-saturated current density and its uniformity evaluated for a circular area 200 mm in diameter [14]. Over a wide range, a uniformity of ±5% or lower was obtained.

Next, a comparison between MSC and SSC is discussed. In the case of SSC, a coil with 0.51 μH inductance was inserted in parallel with an ICP coil to match the impedance. The experiment was conducted using an SSC that can generate sufficiently uniform plasma. The relation between pressure and the ratio of ion-saturated current density of MSC to that of SSC is shown in Figure 22 [15]. The ratio was 2 : 4, indicating that MSC can perform at higher power efficiency over a wide range of discharge conditions. Due to ohmic loss in the parallel coil, the power efficiency of an SSC is lower than that of an MSC.

4.3. Heating the Dielectric Window. It is important not only to suppress particles but also to maintain reproducibility in view of ICP as a mass production tool. To meet these requirements, a heating system was developed for the dielectric window [16]. Figure 23 shows the configuration of this tool. A planar-shaped heating system was installed between the MSC and dielectric window. The heating system consists of two mica plates and a ribbon-shaped heating element in between, with several poles with springs pressing them against the dielectric window. The heating element is a conductor, so it functions as a Faraday shield to prevent erosion of the dielectric window. The heating element is arranged sparsely in the center and with dense circumference, aiming

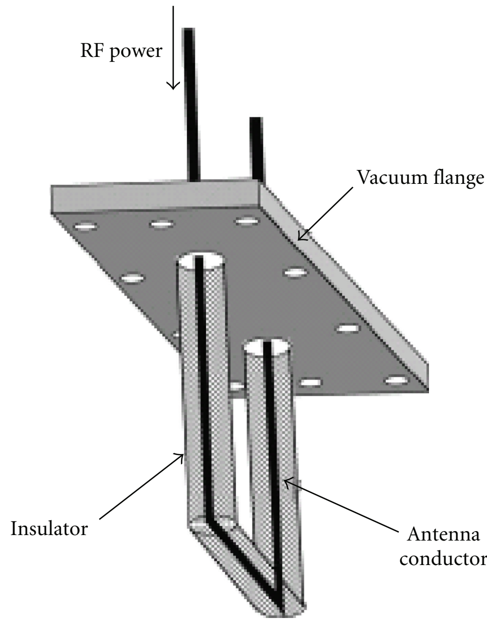

Figure 12: One piece of the many internal coils of large area IC-ICP [12].

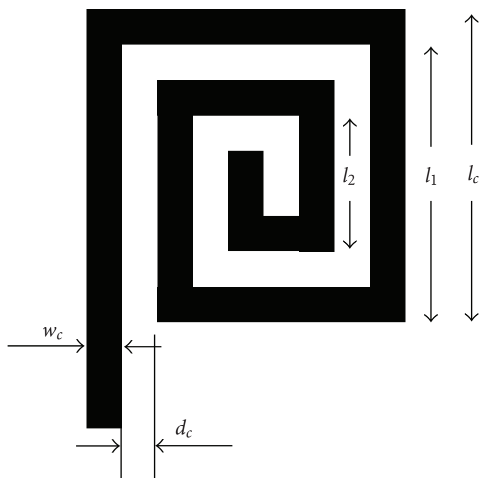

Figure 13: Rectangular single-spiral coil [13].

to compensate the excessive cooling in circumference. In the center of the heating element are noncurrent branches that function as a Faraday shield without generation of heat. There was some concern that RF eddy current at the heating element, which is made of high-resistance metal, might decrease power efficiency in plasma generation, but a sufficient aperture made it possible to maintain efficiency. The temperature of the dielectric window was controlled by getting feedback of the measured value on the side of the window using sheet-shaped thermocouple connected to the controller.

The RF voltage enhanced on the coil is at its maximum in the coil's center. As shown in Figure 23, the coil has three dimensions and is arranged in a cone shape to suppress erosion of the dielectric window by positioning the center of the coil away from the window and decreasing the self-bias voltage on it.

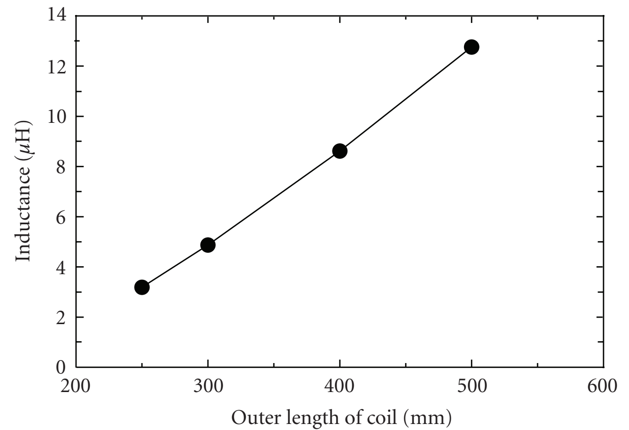

Figure 14: Relation between calculated inductance and the outer length of rectangular SSC.

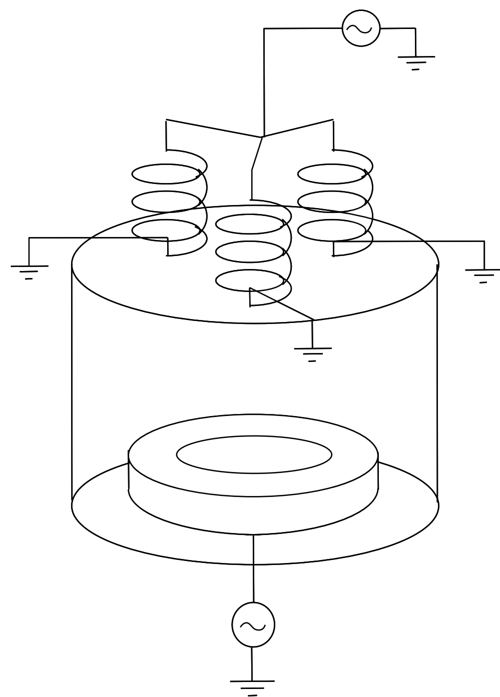

Figure 15: Experimental configuration of plural coils arranged on the dielectric window to form a parallel circuit.

4.4. Symmetrical Chamber Design. In particular processes, uniformity deteriorates because of imbalanced gas flow. For example, in polycrystalline silicon etching using Cl_2, HBr, and O_2 gases, the etching rate tends to be higher near the exhaust. To examine this phenomenon from the viewpoint of plasma generation, a three-dimensional plasma simulation was conducted. The finite volume method code "CFD-ACE+" (CFD Research Corp.), based on a fluid approximation model, enabled CPU time to be saved [28].

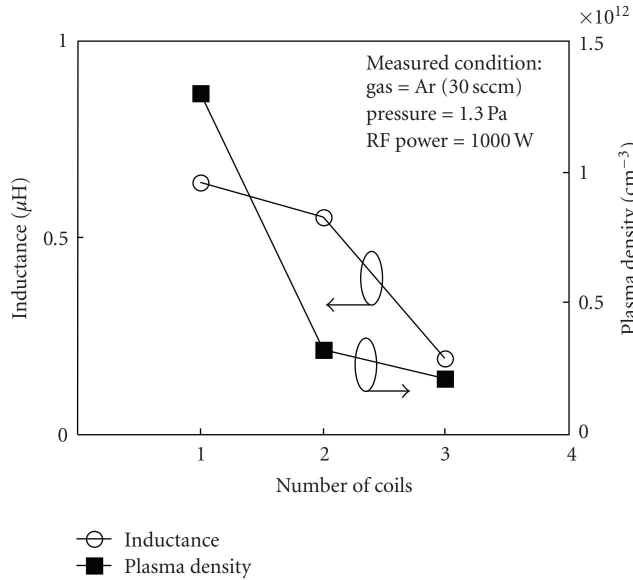

Figure 16: Measured inductance and plasma density and their relation to the number of coils.

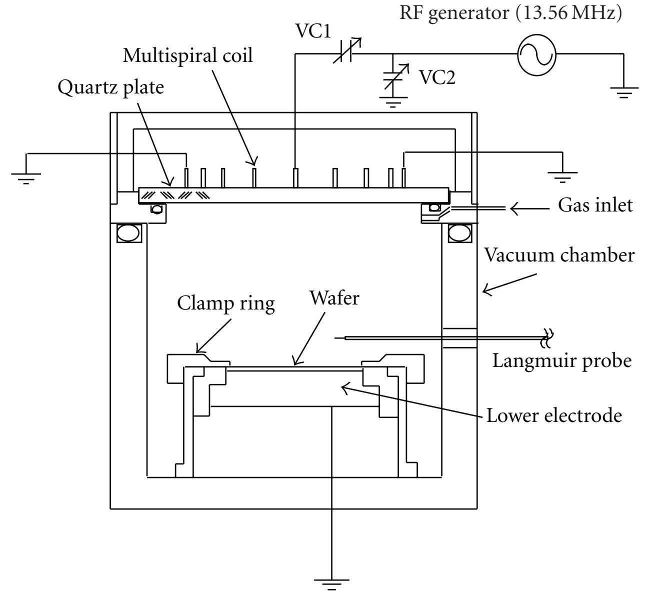

Figure 18: Experimental configuration of MSC-ICP [14].

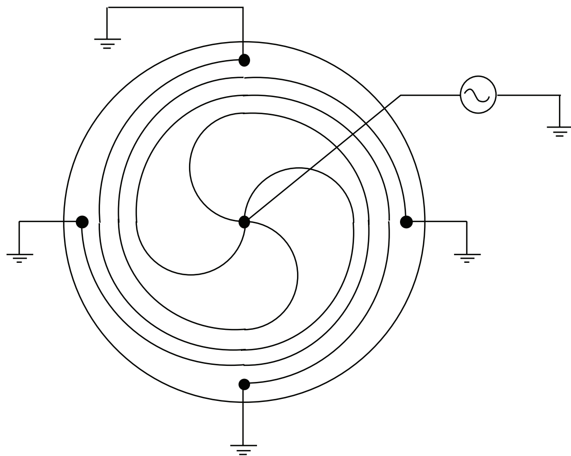

Figure 17: Multispiral coil [14].

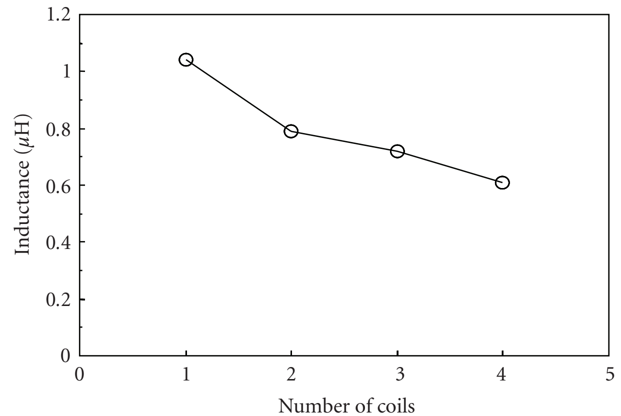

Figure 19: Relation between inductance and number of multiple spiral coils [14].

The gas flow vector simulation results are shown in Figure 24(a) shows the vector in a horizontal section above the lower electrode, while 24(b) shows the vector in a vertical section passing through the center of the lower electrode. This figure reveals that the flow velocity tends to be higher near the exhaust in the case of one-side evacuation. Conversely, the velocity distribution is almost isotropic over the electrode in the case of uniform evacuation although a small whirlpool occurs at the transfer gate.

Electron density and electron temperature simulation results are shown in Figure 25(a), which shows both in a horizontal section above the lower electrode, and figures 25(b) and 25(c) show electron density and electron temperature in a vertical section passing through the center of the lower electrode. This figure reveals that electron density inclines toward the exhaust in the case of one-side evacuation. Electron temperature inclines toward the transfer gate, but the unevenness is very small. Electron density inclines away from the transfer gate, but the unevenness is very small in the case of uniform evacuation.

From these results, it can be assumed that the etching rate near the exhaust tends to be higher in the case of one-side evacuation because the gas exchange is more active and electron density is higher near the exhaust than in other regions.

After the simulation results, an etching tool was developed with perfectly uniform evacuation structure, as shown in Figure 26 [19]. The tool realizes uniform evacuation throughout the circumference by positioning the exhausts around the lower electrode in the same way as in the simulation model, provided that four supports are installed for to float the electrode inside the chamber that is, four exhausts are positioned between each support. Lift pin driving mechanisms for wafer elevation, coolant pipes for

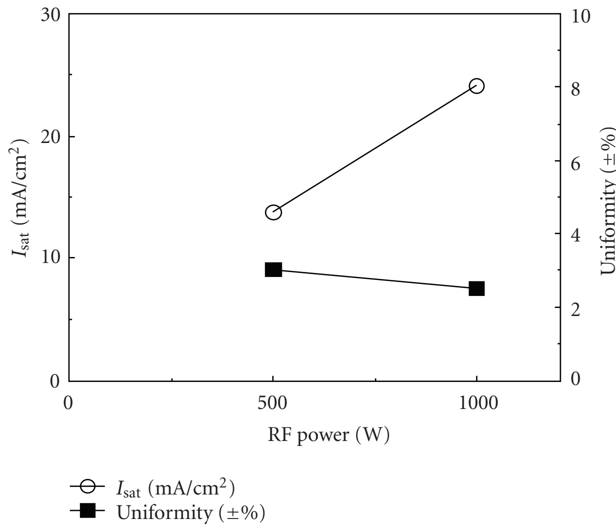

Figure 20: Ion-saturated current density and uniformity and their relation to RF power [14].

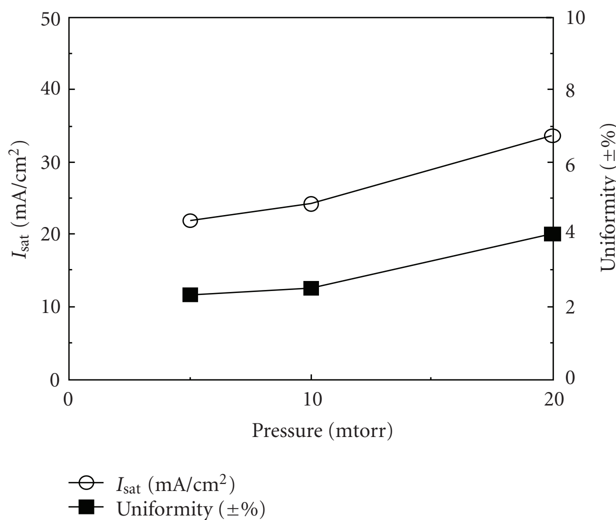

Figure 21: Ion-saturated current density and uniformity and their relation to pressure [14].

electrode temperature control, RF bias lines, and DC lines for an electrostatic chuck (ESC) are accommodated in these supports as well. A vertically driven automatic pressure control valve down below the electrode enables uniform evacuation in any valve position.

4.5. Application to FPDs. Large substrates such as flat panel displays (FPDs) require a large dielectric window. A thicker window is also demanded in order to resist the huge pressure difference between the atmosphere and vacuum, which decreases power efficiency and increases tool costs.

To solve this issue, a coil arrangement was developed that crosses over plural windows set onto plural openings in a metal frame, as shown in Figure 27 [20].

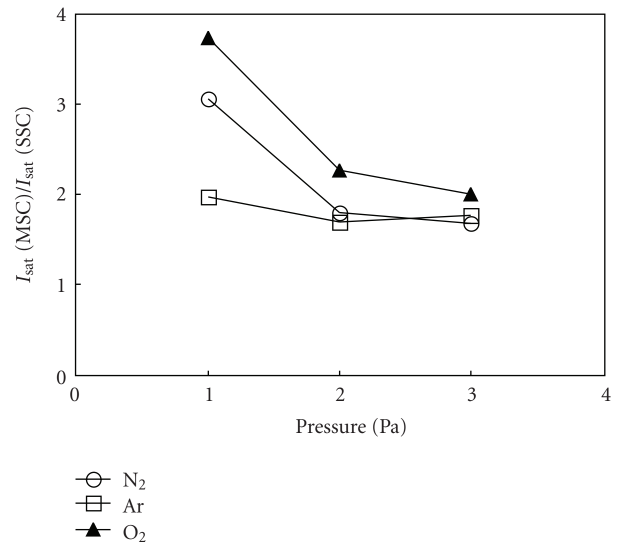

Figure 22: Relation between pressure and the ratio of ion-saturated current density of MSC to that of SSC [15].

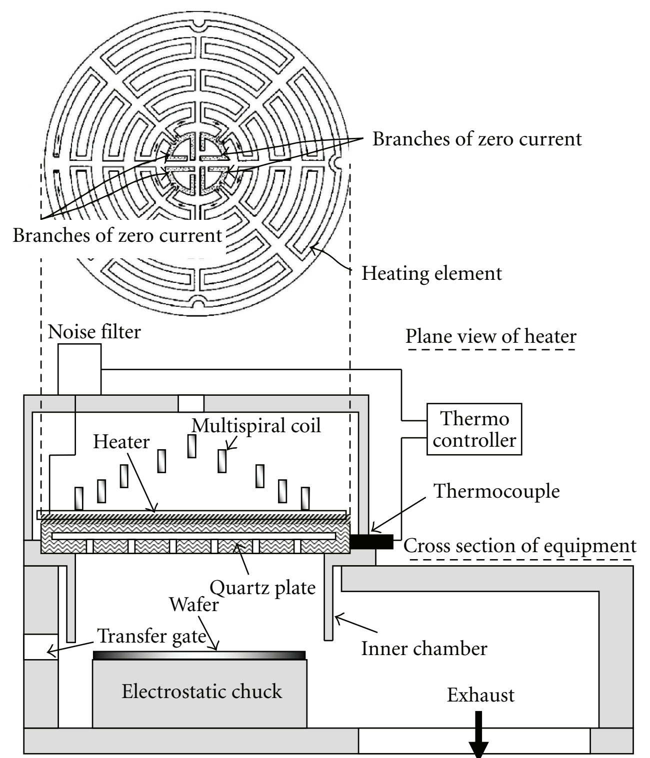

Figure 23: Heating system for the dielectric window in an etching tool [16].

5. Applications of ICP to Various Thin-Film Processing Technologies

ICP etching tools are now widely used in factories producing semiconductors and other various electronic devices.

Figure 28 shows a scanning electron microscopy (SEM) photo of the etched profile of a multilayer of TiN/Al-Si-Cu/TiN/Ti used in back-end processing [15]. The etching

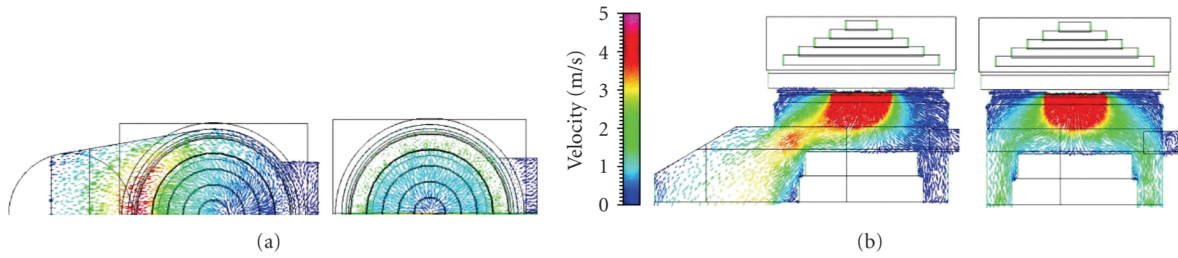

Figure 24: Gas flow vector simulation results: (a) vector in a horizontal section above the lower electrode; (b) vector in a vertical section passing through the center of the lower electrode.

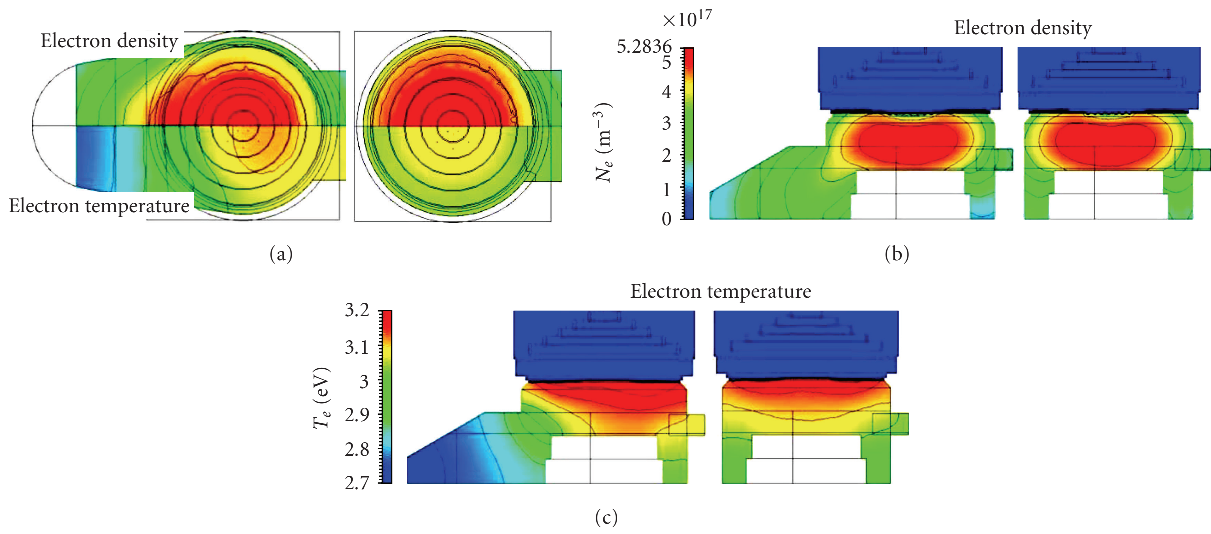

Figure 25: Contour plot of electron density and electron temperature: (a) both in a horizontal section above the lower electrode; (b) and (c) show electron density and electron temperature in a vertical section passing through the center of the lower electrode.

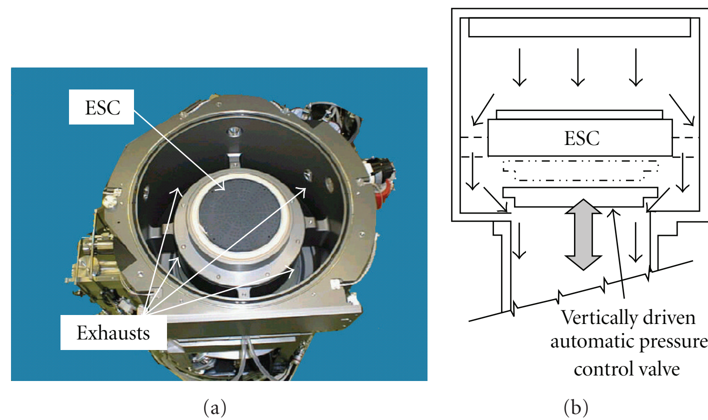

Figure 26: Etching tool with perfectly uniform evacuation structure [19].

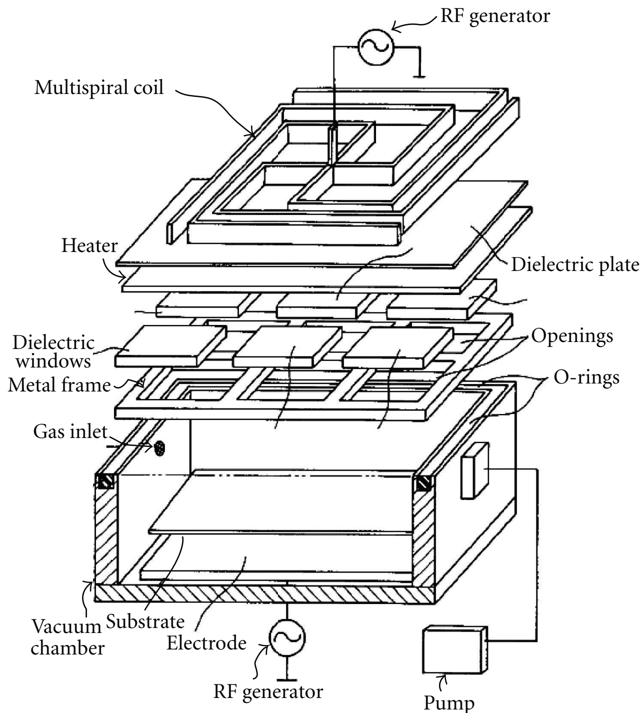

Figure 27: Etching tool for FPDs: coil arrangement crossing over plural windows set onto plural openings in a metal frame [20].

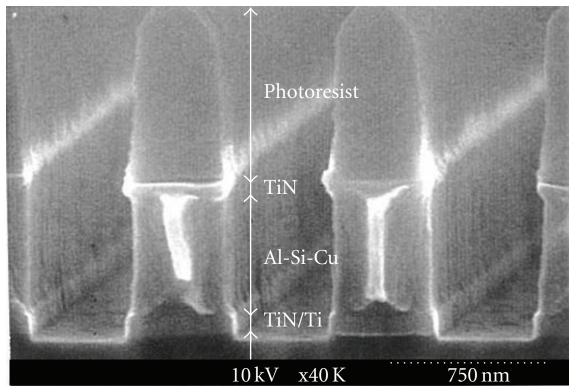

Figure 28: SEM photo of the etched profile of a multilayer of TiN/Al-Si-Cu/TiN/Ti used in back-end processing [15].

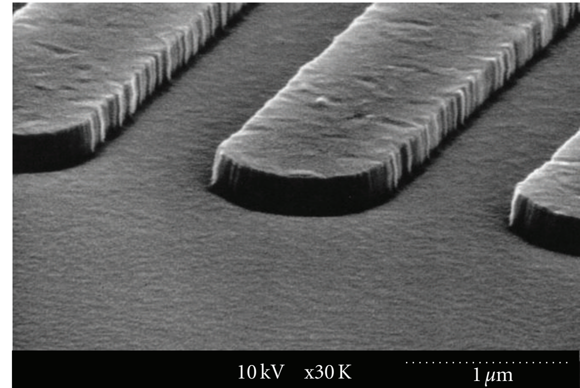

Figure 29: SEM photo of etched Al electrodes of a surface acoustic wave filter [21].

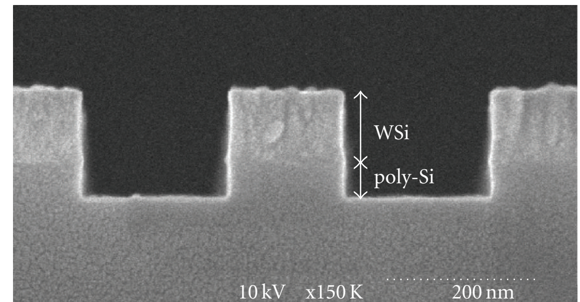

Figure 30: SEM photo of etched polycide gate composed of a multilayer of WSi/poly-Si [22].

rate of the Al-Si-Cu film was 1.1 μm/min. Figure 29 shows an SEM photo of an etched Al electrode of a surface acoustic wave filter [21]. Figure 30 shows an SEM photo of an etched polycide gate composed of a multilayer of WSi/poly-Si [22]. Figure 31 shows an example of silicon trench isolation (STI) [22].

The ICP etching technique is also utilized in the compound semiconductor field. Figure 32 shows a processed via hole of a GaAs power field effect transistor (FET) [22]. The hole depth is 120 μm and etching rate is 5.4 μm/min. Figure 33 shows an example of etched GaN film for high brightness light emitting diodes (LEDs) [23]. The etching rate is 460 nm/min. Figure 34 shows the etched sapphire substrate for a GaN device [23].

ICP is also being used in deep Si etching processes needed in microelectromechanical systems (MEMS) and through silicon via (TSV) methods. Figure 35 shows the result of Si trench etching using the Bosch process, in which etching steps using SF_6 gas and deposition steps using C_4F_8 gas are alternated repeatedly [24]. Figure 36 shows a TSV processed with SF_6 gas [23]. The etching rate here was 20 μm/min.

Processes other than etching also need ICP technology. Figure 37 shows the application result of a gap-fill process, where CVD SiO_2 film was deposited between Al wires [25]. Etching and deposition are simultaneously performed here to fill high aspect ratio gaps by using the so-called bias-CVD process. Figure 38 shows a sheet resistance distribution evaluated after being activated in a plasma doping application [26]. The contour lines are drawn at 5 Ω/sq intervals in the figure. A procedure for using dopant stuck to the dielectric window was invented in the plasma doping process [29].

6. Future Prospects of ICP

Semiconductor miniaturization will soon break through the wall of 10 nm. This size demands not only dimensional accuracy on the scale of several atoms but also controllability of the etching side wall and selectivity to underlayers.

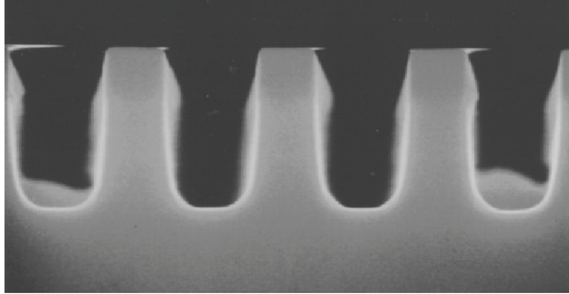

Figure 31: Example of silicon trench isolation (STI) [22].

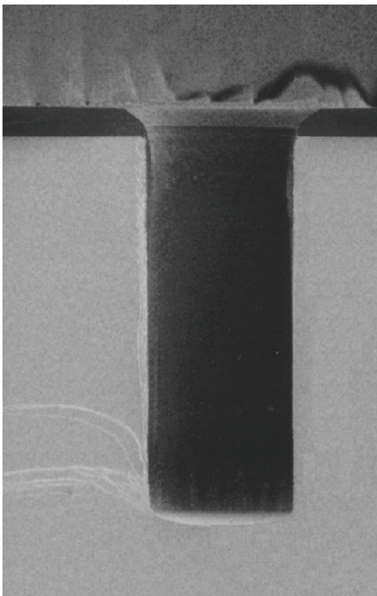

Figure 32: Processed via hole of a GaAs power field effect transistor (FET) [22].

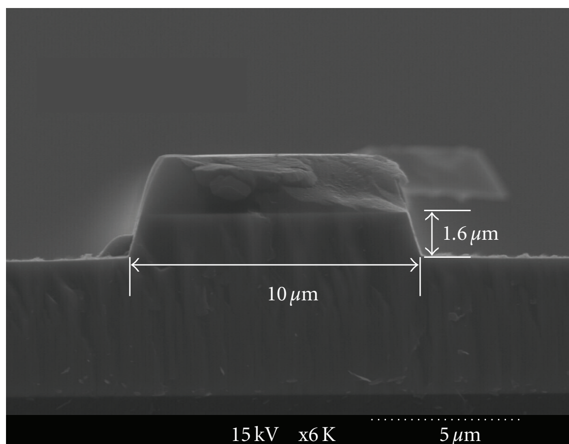

Figure 33: Example of etched GaN film for high brightness light emitting diodes (LEDs) [23].

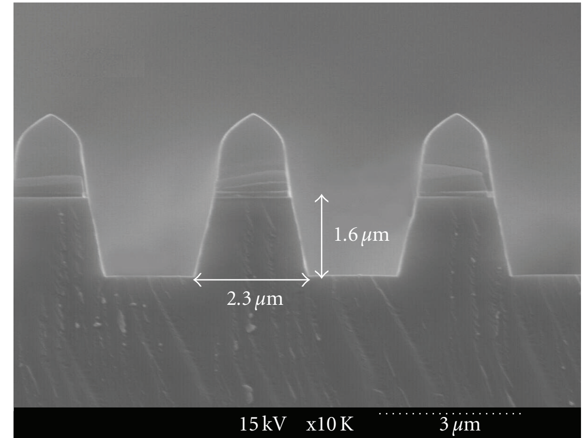

Figure 34: Etched sapphire substrate for a GaN device [23].

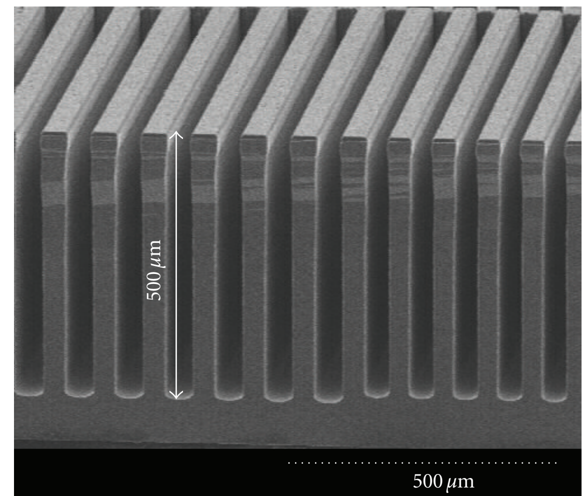

Figure 35: Si trench etching result using the Bosch process [24].

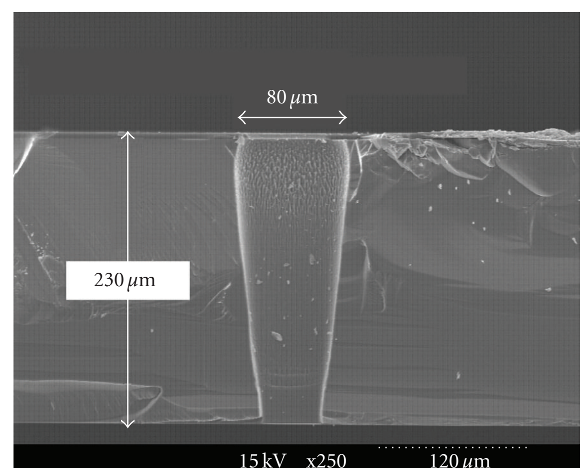

Figure 36: TSV processed with SF_6 gas [23].

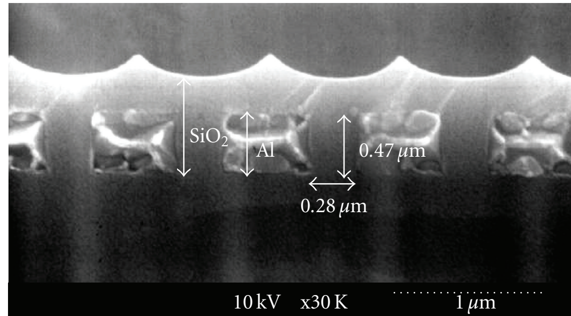

Figure 37: Gap fill CVD process result [25].

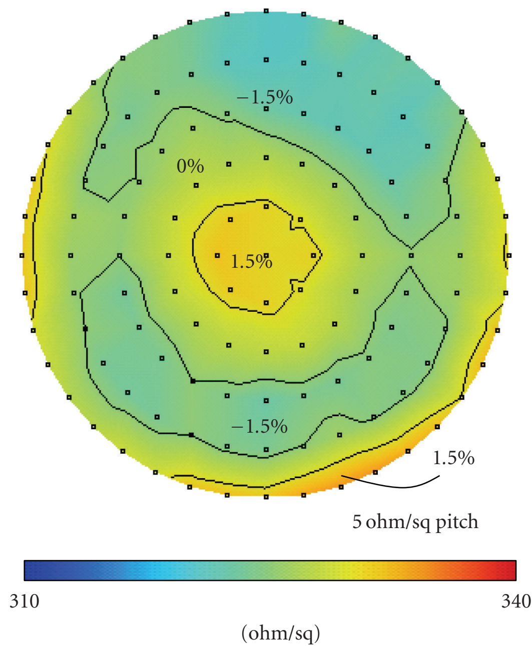

Figure 38: Sheet resistance distribution evaluated in a plasma doping application [26].

To meet these demands, it is necessary to control the plasma parameters more accurately than ever before. Combining precise particle monitoring technology, which can be easily and inexpensively installed in mass production tools, and easy controllability of ICP would work well.

As mentioned in Section 4.5, ICP is being utilized in FPD processes. However, HDP represented by ICP is supposed to be applied only in low-temperature polycrystalline silicon (LTPS) devices, because of the need for finer pattern etching than that possible using amorphous silicon (α-Si) thin-film transistors (TFTs). LTPS devices are now being produced with Generation 4 (G4) substrate dimensions as large as 730 × 920 mm. α-Si TFTs, which deal with G8 substrates 2200 × 2500 mm in dimension, would require ICP technology to meet the demands of high-performance TFTs, needed for three-dimensional and high-precision displays. Therefore, development of ultra large-scale ICP, until now not yet seen, may accelerate.

ICP as an atmospheric plasma source is undergoing continuous innovation. As described in Section 3, this technique has long been used for plasma spray coating. Recently developed has been rapid thermal processing (RTP) for thin films, in which an ICP torch is used as a heat source. The ICP torch is scanned at high speed, and polycrystalline silicon film can be acquired by heating the α-Si film over a very short period of time, on the order of ms [30]. This process has advantages of lower tool costs and lower operating costs compared to laser annealing, with further improvements expected in the future. Recent years have seen rapid progress in research and development of atmospheric plasma, which is sure to yield many innovative applications combining conventional ICP and new discoveries.

References

[1] J. Hopwood, “Review of inductively coupled plasmas for plasma processing,” *Plasma Sources Science and Technology*, vol. 1, no. 2, pp. 109–116, 1992.

[2] T. Yoshida, “Future of thermal plasma processing,” *Transactions of the Japan Institute of Metals*, vol. 30, no. 1, pp. 1–11, 1990.

[3] S. Takechi and S. Shinohara, “Role of electron thermal motion in evanescent electromagnetic wave structure of inductively coupled plasma,” *Japanese Journal of Applied Physics*, vol. 38, no. 2 A, pp. L148–L150, 1999.

[4] J. Hopwood, C. R. Guarnieri, S. J. Whitehair, and J. J. Cuomo, “Langmuir probe measurements in an rf induction plasma,” *Journal of Vacuum Science & Technology A*, vol. 11, pp. 152–156, 1993.

[5] J. S. Ogle, “Method and apparatus for producing magnetically-coupled planar plasma,” US patent 4948458, 1990.

[6] L. J. Mahoney, A. E. Wendt, E. Barrios, C. J. Richards, and J. L. Shohet, “Electron-density and energy distributions in a planar inductively coupled discharge,” *Journal of Applied Physics*, vol. 76, no. 4, pp. 2041–2047, 1994.

[7] M. Edamura, K. Yoshioka, R. Nishio et al., “A novel plasma etching tool with rf-biased Faraday-shield technology: chamber surface reaction control in the etching of nonvolatile materials,” *Japanese Journal of Applied Physics*, vol. 42, no. 12, pp. 7547–7551, 2003.

[8] Y. Kokaze, I. Kimura, T. Jimbo, M. Endo, M. Ueda, and K. Suu, “Coating and etching technologies for piezoelectric and ferroelectric MEMS,” *ULVAC Technical Journal*, vol. 66E, pp. 13–19, 2007.

[9] G. Vinogradov, V. Menagarishvili, A. Kelly, and Y. Hirano, “Advanced dielectric etch using 200/300-mm low residence time GrovyICP™ etcher,” in *Proceedings of the 206th Meeting of the Electrochemical Society*, p. 899, October 2004.

[10] J. Hoang, C. C. Hsu, and J. P. Chang, “Feature profile evolution during shallow trench isolation etch in chlorine-based plasmas. I. Feature scale modeling,” *Journal of Vacuum Science and Technology B*, vol. 26, no. 6, pp. 1911–1918, 2008.

[11] K. Nakamura, Y. Kuwashita, and H. Sugai, “New inductive rf discharge using an internal metal antenna,” *Japanese Journal of Applied Physics*, vol. 34, no. 12 B, pp. L1686–L1688, 1995.

[12] Y. Setsuhara, “Meter-scale large-area plasma sources for next-generation processes,” *Journal of Plasma and Fusion Research*, vol. 81, pp. 85–93, 2005.

[13] K. I. Arai, “Applied magnetics 3,” *Journal of the Magnetics Society of Japan*, vol. 24, pp. 1198–1203, 2000.

[14] T. Okumura and I. Nakayama, "New inductively coupled plasma source using a multispiral coil," *Review of Scientific Instruments*, vol. 66, no. 11, pp. 5262–5265, 1995.

[15] T. Okumura, I. Nakayama, A. Mitsuhashi, and H. Suzuki, "Large area inductively coupled plasma source for dry etching," in *Proceedings of the 131st Committee on Thin Film*, pp. 20–24, The Japan Society for the Promotion of Science, 1995.

[16] T. Okumura, S. Watanabe, H. Haraguchi, and I. Nakayama, "Method and device for plasma treatment," US patent 6177646, 2001.

[17] J. Hopwood, "Planar RF induction plasma coupling efficiency," *Plasma Sources Science and Technology*, vol. 3, no. 4, pp. 460–464, 1994.

[18] K. Yoshida, H. Miyamoto, E. Ikawa, and Y. Murao, "Gate electrode etching using a transformer coupled plasma," *Japanese Journal of Applied Physics*, vol. 34, pp. 2089–2094, 1995.

[19] T. Kimura, T. Okumura, and M. Yoshinaga, "New dry etching technology," *Matsushita Technical Journal*, vol. 47, pp. 18–22, 2001.

[20] Y. Yanagi, I. Nakayama, and T. Okumura, "Plasma processing method and apparatus," Japan Patent 3729939, 2005.

[21] T. Okumura, A. Mitsuhashi, and Y. Tanaka, "High density plasma dry etching technology capable of processing 0.25 μm rule devices," *National Technical Reports*, vol. 43, pp. 19–25, 1997.

[22] T. Okumura, *Handbook of Ion Sources*, CRC Press, New York, NY, USA, 1995.

[23] H. Suzuki and S. Okita, "Development of high-production dry etching process technology for MEMS and LED devices," *Panasonic Technical Journal*, vol. 55, pp. 63–65, 2009.

[24] Panasonic Factory Solutions, "Etching equipments," MEMS Technology, Outlook, pp. 413–418, 2008.

[25] T. Okumura, K. Arai, I. Nakayama, K. Sawada, and Y. Yamada, "Interlayer insulating film formation using multi-spiral coil ICP source," in *Proceedings of the 43rd Spring Meetings*, The Japan Society of Applied Physics and Related Societies, 1995, 30a-C-8.

[26] Y. Sasaki, H. Ito, K. Okashita et al., "Production-worthy USJ formation by self-regulatory plasma doping method," in *Proceedings of the the 16th International Conference on Ion Implantation Technology (IIT '08)*, p. 188, 2008.

[27] S. Adachi, *Engineering of Electromagnetic Waves*, vol. 41, Corona Publishing Co. Ltd., 1983.

[28] K. Ikeda, T. Okumura, and V. Kolobov, "Three dimensional simulation for inductively coupled plasma reactor employing multi-spiral coil," *Journal of the Vacuum Society of Japan*, vol. 50, no. 6, pp. 424–428, 2007.

[29] T. Okumura, I. Nakayama, and B. Mizuno, "Method of plasma doping," US patent 7575987, 2009.

[30] M. Ryo, Y. Sakurai, T. Kobayashi, and H. Shirai, "Rapid recrystallization of amorphous silicon utilizing very-high-frequency microplasma jet at atmospheric pressure," *Japanese Journal of Applied Physics*, vol. 45, no. 10 B, pp. 8484–8487, 2006.

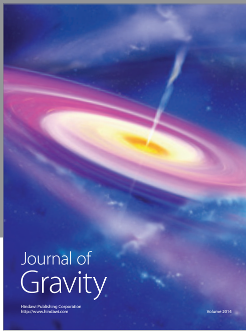
Journal of
Gravity
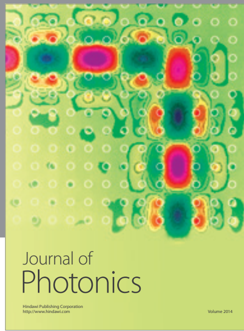
Journal of
Photonics

The Scientific
World Journal

Journal of
Soft Matter
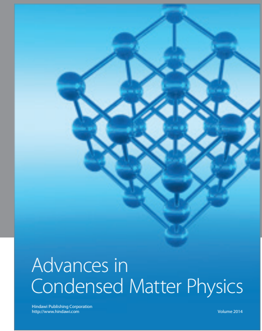
Advances in
Condensed Matter Physics

Journal of
Fluids

Hindawi
Submit your manuscripts at
http://www.hindawi.com
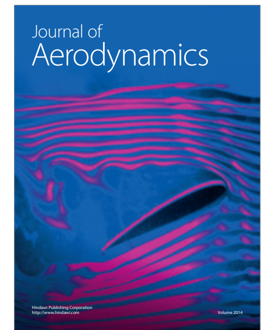
Journal of
Aerodynamics

International Journal of
Statistical Mechanics
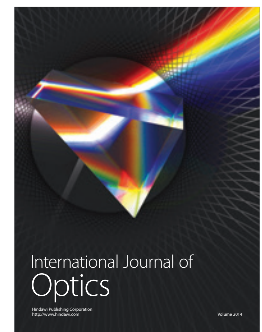
International Journal of
Optics
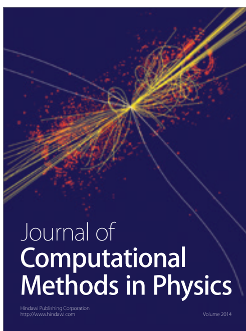
Journal of
Computational
Methods in Physics
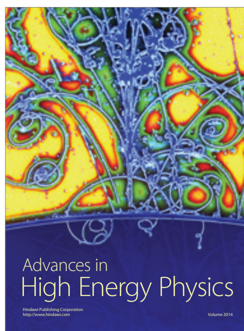
Advances in
High Energy Physics

Journal of
Thermodynamics
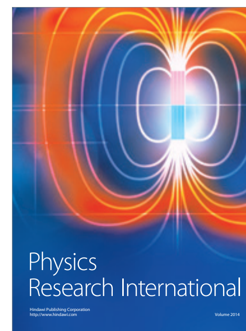
Physics
Research International
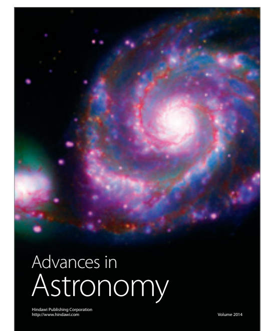
Advances in
Astronomy

Journal of
Solid State Physics

Journal of
Astrophysics

International Journal of
Superconductivity

Journal of
Biophysics
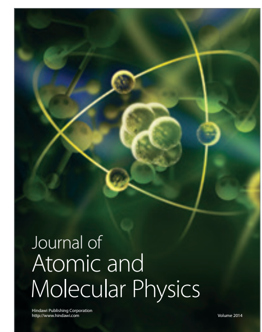
Journal of
Atomic and
Molecular Physics